Rare Metal Materials and Engineering
Volume 52, Issue 8, August 2023
Available online at www.rmme.ac.cn

Science Press

Cite this article as: Chen Shanshan, Liu Zongde, Pan Chaoyang, et al. High-Temperature Oxidation and Hot Corrosion Characteristics of Ni-Cr Alloy Cladding Layers with Different Cr Contents[J]. Rare Metal Materials and Engineering, 2023, 52(08): 2702-2710.

ARTICLE

High-Temperature Oxidation and Hot Corrosion Characteristics of Ni-Cr Alloy Cladding Layers with Different Cr Contents

Chen Shanshan, Liu Zongde, Pan Chaoyang, Liu Fulai, Fu Yundi

Key Laboratory of Power Station Energy Transfer Conversion and System, Ministry of Education, North China Electric Power University, Beijing 102206, China

Abstract: Ni-Cr alloy cladding layers with Cr contents of 10wt%, 20wt%, and 40wt% were prepared by laser melting technique and their high temperature oxidation characteristics at 900 °C and hot corrosion characteristics in Na_2SO_4+25wt% K_2SO_4 mixed salt at 600 °C were investigated. The results show that the Cr content plays a key role in the high temperature characteristics of cladding layers. Increasing the Cr content is more effective in improving the resistance of cladding layers to sulfate-induced hot corrosion than in improving the resistance to cyclic high-temperature oxidation. Cr40 provides the best resistance to high-temperature oxidation and hot corrosion. The oxidation products of Cr10 are dominated by NiO, which is extremely easy to shed and the internal oxidation is serious. Although a single Cr_2O_3 layer can be formed on the Cr40 surface, cracking within the Cr-rich oxides caused by thermal and growth stresses renders the resistance of Cr40 to cyclic high-temperature oxidation only slightly better than that of Cr20. Suffering from hot corrosion, the surface of Cr10 presents lamellar NiO and Ni_3S_2 stacked distribution of corrosion products, and Ni sulfide is also generated in the inner corrosion zone. The Cr_2O_3 layer on Cr20 surface is destroyed, and internal corrosion is severe, generating CrS. A dense protective Cr_2O_3 layer is generated on Cr40 surface, efficiently preventing further corrosion.

Key words: Ni-Cr alloy; laser cladding technology; high-temperature oxidation; high-temperature sulfate corrosion

Thermal power generation is an important pillar of the energy and power industry. So far, the main method of thermal power generation is still coal-fired power generation. With the rapid development of society, to meet the needs of sustainable development of resources and protection of the ecological environment, and to improve the operating efficiency of coal-fired power generation units, supercritical and ultra-supercritical units have become the main development trend of new and expanded units. Therefore, the requirements for the performance of boiler tube materials for thermal power units are getting higher and higher, which requires them to work at higher temperatures and harsher environmental conditions[1–6]. Nickel-based alloys are important corrosion-resistant materials, and the effect of their corrosion resistance comes from the stability of the passive film formed on the surface of nickel-based alloys. Compared with the general stainless steel, other corrosion resistant metal and non-metallic materials, nickel-based alloy in a variety of corrosive environments including electrochemical corrosion and chemical corrosion has the ability to resist various forms of corrosion damage (including general corrosion, localized corrosion and stress corrosion, etc), with both good mechanical properties and processing performance. Therefore, nickel-based alloys are excellent candidates for boiler tubes serving in harsher environments [7–9].

Ni is a face-centered cubic structure, the structure is very stable, and there is no allotropic transformation from room temperature to high temperature. It has good alloying ability, which provides a variety of possibilities for improving the properties of Ni-based alloys[10–12]. After adding a certain amount of Cr to the Ni-based alloy, a dense Cr_2O_3 layer can be formed on the surface of the alloy at high temperature, which gives the alloy better resistance to high temperature oxidation and hot corrosion. However, the resources of Ni are valuable and the cost is high, which limits the wide application of Ni-based alloys. Laser cladding technology can prepare crack-free, hole-free cladding layer with low dilution rate and metallurgical bonding with the substrate. It can greatly improve the wear resistance, corrosion resistance, oxidation

Received date: January 21, 2023
Corresponding author: Liu Zongde, Ph. D., Professor, Key Laboratory of Power Station Energy Transfer Conversion and System, Ministry of Education, North China Electric Power University, Beijing 102206, P. R. China, Tel: 0086-10-61771025, E-mail: lzd@ncepu.edu.cn

resistance and other properties of the surface of the substrate material[13]. Using laser cladding technology to deposit a Ni-Cr alloy cladding layer on the surface of the substrate cannot only obtain high temperature oxidation and corrosion resistance similar to the alloy with the same composition, but also achieve effective protection of engineering components and greatly reduce the cost. Therefore, the use of laser cladding technology for high temperature corrosion protection of boiler tubes have been widely concerned[14–17].

Increasing the Cr content of nickel-based superalloys can significantly improve the high temperature oxidation resistance of the alloy, and also reduce the Ni content in the alloy to reduce the production cost. But the content of Cr in the alloy should not be too high, otherwise it will lead to brittle alloy and decrease high temperature strength. Adding an appropriate amount of Cr cannot only make the alloy have good high temperature resistance but also maximize its functional properties[18–20]. Therefore, a large number of scholars have studied the high temperature oxidation resistance and hot corrosion resistance of Ni-20Cr alloy. However, systematic studies on laser cladding layers of Ni-Cr alloys with low or high Cr content are less reported. In this work, three Ni-Cr alloys with Cr content of 10wt%, 20wt% and 40wt% were selected as cladding layer materials, and their high temperature oxidation and hot corrosion properties were tested. The mechanism of high temperature oxidation and sulfate corrosion resistance of Ni-Cr alloy cladding layers with three different Cr contents were studied to figure out the influence of Cr content on the high temperature properties, so as to provide a basis for promoting the application of Ni-Cr alloy laser cladding layers in high temperature corrosion protection of boiler tubes.

1 Experiment

1.1 Preparation of materials

First, pure Cr powder were added to pure Ni powder, and three kinds of Ni-Cr powders with 10wt%, 20wt% and 40wt% Cr were obtained after constant stirring for 10 h; second, three different Ni-Cr alloy cladding layers were prepared on Q235 steel plate by laser cladding technology, named as Cr10, Cr20 and Cr40, respectively. In order to avoid the influence of the diffusion of matrix elements into the cladding layer on the experimental results, the cladding layer with a total thickness greater than 4.5 mm was obtained by multi-layer cladding. The sample was taken at the upper part of the cladding layer and cut to obtain the experimental sample with a size of 20 mm×10 mm×2 mm. Using 400#, 600#, 800#, 1000# waterproof sandpaper to grind surface so as to eliminate the influence of surface roughness on the accuracy of experimental results. Finally, the samples were subjected to ultrasonic vibration cleaning for 10 min with anhydrous ethanol solution and acetone solution to remove the surface oil and impurities, and then dried.

1.2 High temperature oxidation experiment

In this work, the tubular resistance furnace was used as the heating equipment, the air was used as the experimental atmosphere, and the experimental temperature was constant at 900 °C. Before the experiment, the initial surface area (A) and initial mass (including the mass of the crucible) of each sample were measured. Then the high temperature oxidation experiment was carried out. A cycle was 24 h. The sample was taken out and cooled to room temperature, and weighed together with the crucible to obtain the mass change (Δm) in a cycle. Then the sample was put into the furnace again to continue the next cycle of oxidation, and the above operation was repeated. The longest oxidation time was 144 h (6 cycles). The growth rate of oxidation products on the surface of the cladding layer can be expressed by the mass change per unit area, that is, the oxidation resistance of the cladding layer was measured by the formula $\Delta w = \Delta m/A$, where Δw is the mass variation per unit area of the cladding layer (mg/cm^2).

1.3 High temperature sulfate corrosion experiment

Hot corrosion experiments were still carried out in the air, tube resistance furnace was heating equipment, and the two salts were mixed evenly with Na_2SO_4:K_2SO_4=3:1 (mass fraction ratio). High temperature corrosion test was conducted at 600 °C. The treated and weighed cladding layer samples were placed in a crucible together with a certain amount of mixed salt, and then the remaining space in the crucible was filled with salt to ensure that the samples were completely buried. The corrosion experiment adopted a non-cyclic method, that is, the sample was continuously corroded in the mixed salt for 144 h.

Since the corrosion products were easy to fall off, the mass loss per unit area was used to measure the high temperature sulfate corrosion resistance of the cladding layer. Therefore, there was one more pickling step than the high temperature oxidation experiment (the purpose of pickling was to remove the surface corrosion products). The pickling process was as follows: the sample was taken out and cooled to room temperature, the residual salt and some corrosion products on the surface were ultrasonically cleaned with deionized water, and ultrasonic cleaning with 25 wt% sulfuric acid at 80 ° C was performed to completely remove the corrosion products on the surface of the sample; the sample was weighed after fully drying.

1.4 Characterization method

The microstructure of the three cladding layers was observed by scanning electron microscope (SEM). The main phase composition, oxidation products and corrosion products of the cladding layer were determined by X-ray diffractometer (XRD). The surface and cross-section morphology of the oxidation and corrosion products of the cladding layer after high temperature oxidation and hot corrosion were observed by SEM, and the main element distribution at typical locations was analyzed by energy dispersive X-ray spectroscopy (EDS).

2 Results and Discussion

2.1 Microstructure and phase composition of the cladding layer

Fig.1 shows the XRD patterns of the three cladding layers,

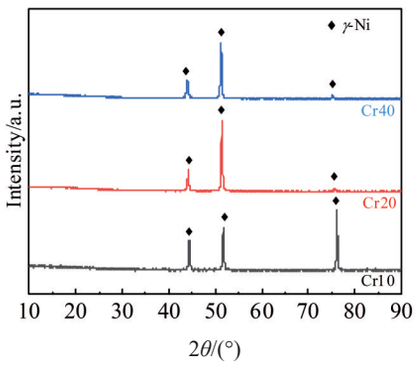

Fig.1 XRD patterns of three Ni-Cr alloy cladding layers

Cr10, Cr20 and Cr40. It can be seen that the main phase composition of the three cladding layers is almost the same, all consisting of γ-Ni solid solution which can be regarded as Cr solid solution into the lattice of γ-Ni. Accordingly, the microstructures of the three cladding layers are also similar. The SEM microstructures after aqua regia erosion are shown in Fig.2. The clear grain boundary structure can be observed. No obvious precipitation phase is found.

2.2 High temperature oxidation properties

2.2.1 Oxidation products and oxidation mass gain per unit area

The XRD analysis results of oxidation products of the three cladding layers after cyclic oxidation test at 900 °C (144 h) are shown in Fig.3a, and γ-Ni solid solution is detected in all the three samples. After high-temperature oxidation test at 900 °C, NiO and $NiCr_2O_4$ form on the surface of Cr10, Cr_2O_3, NiO and $NiCr_2O_4$ are detected on the surface of Cr20, and Cr40 almost only produces Cr_2O_3.

The mass gain per unit area of the cladding layer after cyclic oxidation at 900 °C is shown in Fig.3b. The oxidation mass gain of Cr10 exhibits a continuous growth trend with the extension of time, almost a linear trend, because the low Cr content in Cr10 results in the formation of dense Cr_2O_3 layer. The oxides generated during the oxidation process continuously crack and expose new surfaces, which cannot isolate O_2. However, the oxidation mass gain per unit area of Cr20 and Cr40 is significantly lower than that of Cr10, showing excellent high-temperature oxidation resistance. The oxidation kinetics curves of the two cladding layers follow similar trends. With the extension of time, the oxidation rate tends to be stable in general, and the oxides grow slowly. Usually, the oxidation process of metals can be divided into three stages. First, the gas adsorbed on the metal surface reacts with metal atoms to generate oxide films. In this stage, the oxidation rate (thickening of the oxide film) changes greatly with time. Second, after the formation of oxide films on the surface, the oxygen molecules in gas phase are adsorbed on the surface of the oxide film, decomposed and ionized into O^{2-}, and migrate to the oxide/metal interface. At the same time, the cations in the metal move towards the air/oxide interface. Third, at the oxide/metal interface, metal ions interact with O_2 to form oxides, which continue to thicken the oxide film. The oxidation kinetics of Cr20 and Cr40 presents a

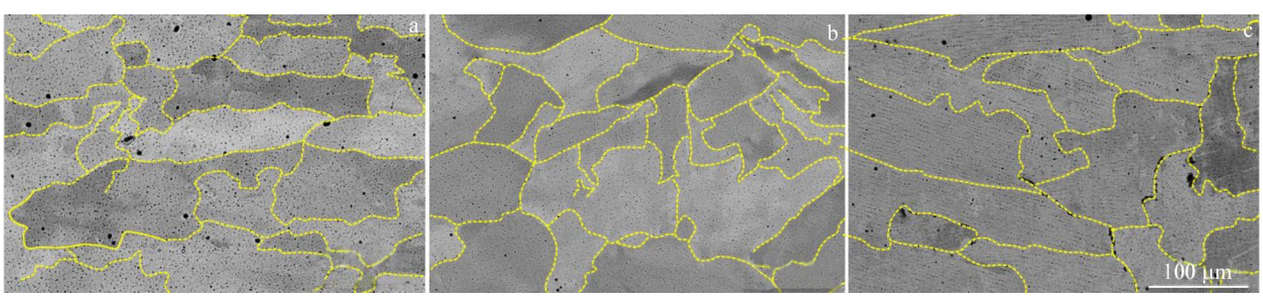

Fig.2 SEM microstructures of three Ni-Cr alloy cladding layers: (a) Cr10, (b) Cr20, and (c) Cr40

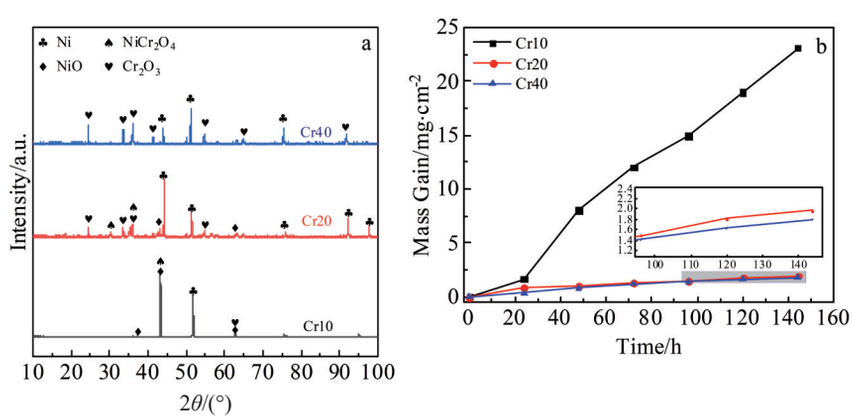

Fig.3 XRD patterns of oxidation products (a) and oxidation mass gain at 900 °C per unit area (b)

parabola law, indicating that the Cr_2O_3 dominated oxide layer formed on the surface of two cladding layers can well hinder the second and third stages of oxidation, and provide excellent protection.

2.2.2 Surface morphology of oxidation products

The surface morphologies of the oxidation products of Cr10, Cr20 and Cr40 are shown in Fig. 4 and the results of EDS analysis of typical locations are shown in Table 1. The surface oxidation products of Cr10 have two characteristics, one is a dense icing sugar-like oxidation product, and the other is a loose oxidation product which has a large surface peeling. In combination with the EDS and XRD results, the icing sugar-like oxidation product is NiO, which is attached to the surface of the sample, and the oxidation product to be peeled off mainly consists of Ni, Cr and O. It is inferred that $NiCr_2O_4$ is generated at this location. As can be clearly seen from the oxidation kinetic curves, the Cr10 surface oxide layer cannot effectively prevent the continuation of the oxidation reaction. As the Cr content increases, no icing-like NiO layer is found in the surface oxidation products of Cr20 and Cr40, which both generate Cr_2O_3 (areas 4, 6 and 7) as well as $NiCr_2O_4$, (areas 3, 5 and 8). This is due to the fact that the affinity between Cr and O is much higher than that between Ni and O. Therefore, when the Cr content is high enough, Cr_2O_3 is formed preferentially at the beginning of oxidation, and gradually a continuous Cr-rich oxide layer forms on the surface. The Ni content in the Cr20 surface oxidation products is still high, dominated by $NiCr_2O_4$, and Cr_2O_3 can be observed at the exfoliated position. While the Cr40 surface oxidation products are heterogeneous, dominated by Cr_2O_3, but it is distributed with layers of smooth $NiCr_2O_4$, probably because the Cr-rich oxide has been exfoliated at this location. In fact, there are growth stresses and thermal stresses in the oxide layer formed on the surface of the molten cladding layer. During the holding process of this experiment, the stresses generated during the growth of the Cr-rich oxide layer are generative stresses. Since it is a cyclic oxidation test, there is a drastic temperature change when the sample is removed, and the stress is generated due to different coefficients of linear expansion between different oxides and between the oxide and the metal should be thermal stress. As a result, the oxide layer is easily peeled off, which affects the high temperature oxidation resistance.

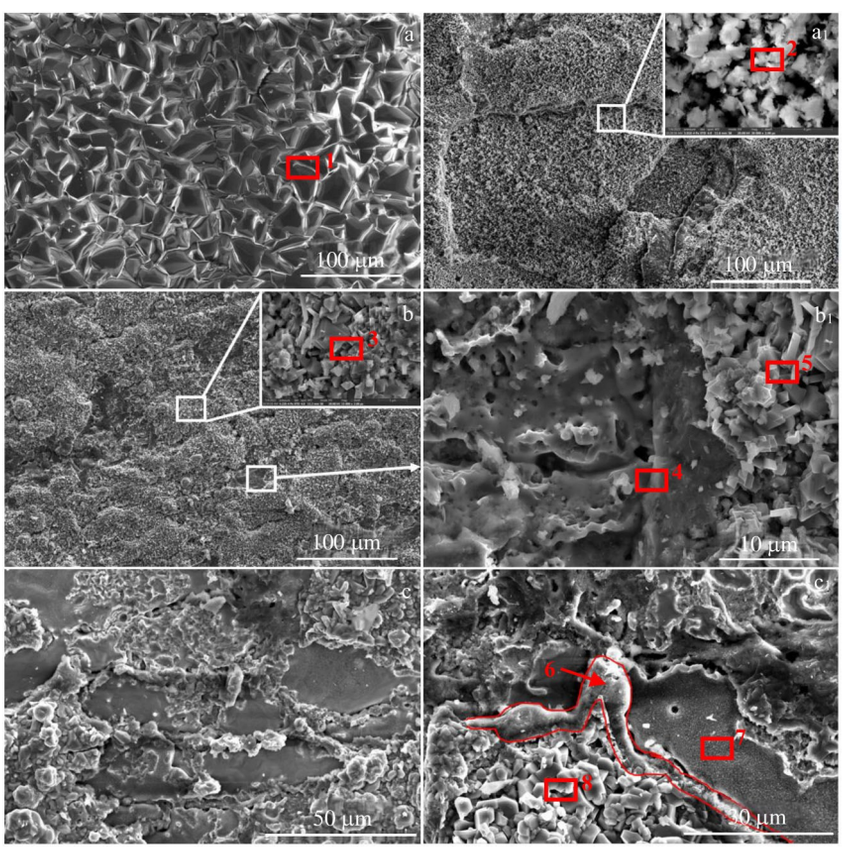

Fig.4 Surface morphologies of the oxidation products of three Ni-Cr alloy cladding layers: (a, a_1) Cr10, (b, b_1) Cr20, and (c, c_1) Cr40

Table 1 EDS results of different areas in Fig.4 (wt%)

Area	1	2	3	4	5	6	7	8
O	62.6	38.6	44.8	8.3	41.3	40.9	18.7	44.1
Ni	36.0	25.8	19.6	5.7	22.6	1.7	56.3	1.3
Cr	1.3	35.7	35.6	86.0	36.0	57.4	25.0	54.6

2.2.3 Cross-sectional morphology of oxidation products

Fig. 5 shows the cross-sectional characteristics of three Ni-Cr alloy cladding layers after 900 °C high temperature cyclic

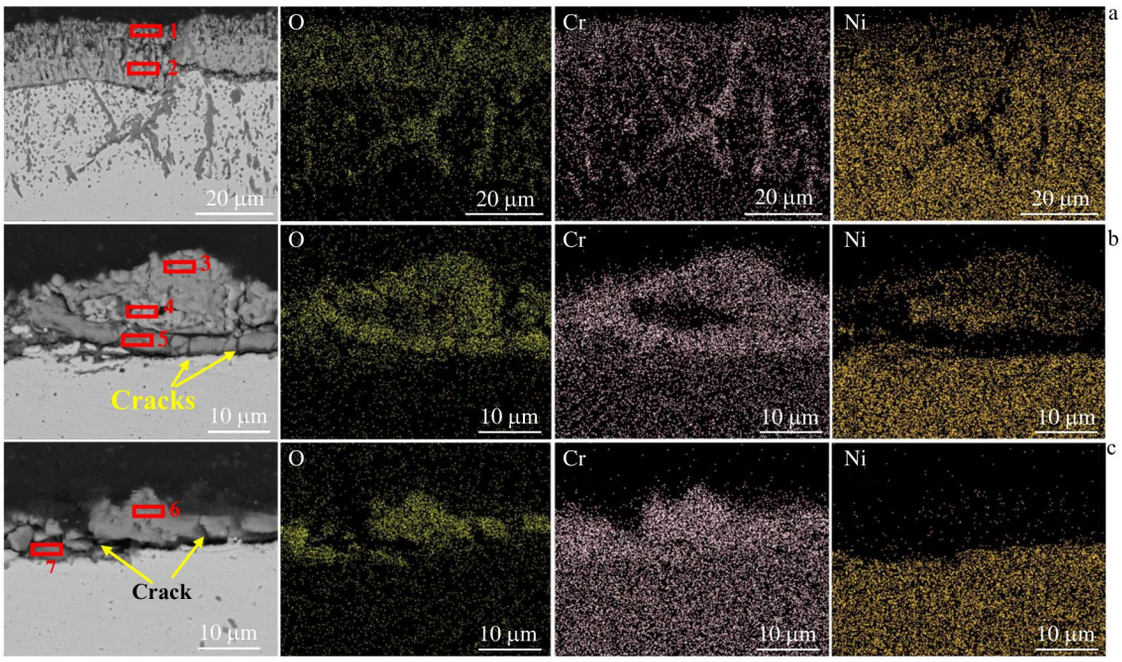

Fig.5 Cross-sectional characteristics and EDS element mappings of three Ni-Cr alloy cladding layers: (a) Cr10, (b) Cr20, and (c) Cr40

oxidation. The corresponding EDS analysis results are shown in Table 2. Unlike the other two molten clad layers, Cr10 shows severe internal oxidation due to its low Cr content, and the initial formation of Cr_2O_3 makes it difficult to form a continuous Cr-rich oxide layer due to insufficient Cr supply, resulting in a NiO-dominated final oxide on the surface. The inward diffusion of O is not effectively prevented, resulting in the formation of rod-like internal oxides (Cr_2O_3) inside Cr10. As can be seen in Fig. 5b, as the Cr content is elevated to 20wt% , two layers of oxide products are formed on the surface of the Cr20 fused layer, the outer layer is mainly $NiCr_2O_4$ and the lower layer is dominated by Cr_2O_3, which is consistent with the information fed by the surface morphology, but a piece of NiO is also sandwiched between the two layers. Compared with Cr10, the Cr_2O_3 content in the Cr20 surface oxide products increases. As the oxidation proceeds, due to the continuous outward diffusion of Ni and the faster growth of NiO, the slower-growing Cr_2O_3 is gradually covered to form the inner and outer oxide layers, and the solid-state reaction between NiO and Cr_2O_3 gradually occurs to produce $NiCr_2O_4$. In addition, almost no internal corrosion zone is found on Cr20, indicating that the Cr-rich oxide film on the surface of Cr20 hinders the inward diffusion of O, but fails to effectively prevent outward diffusion of Ni. In fact, since cations diffuse through Cr_2O_3 and $NiCr_2O_4$ is much slower than through NiO, these Cr_2O_3 and $NiCr_2O_4$ in the oxide layer act as a barrier to the outwardly migrating Ni^+. Therefore, when the Cr content reaches 40wt%, a dense Cr_2O_3-dominated oxide layer is formed on the surface of Cr40, and from the EDS mapping results, the oxide layer contains almost no Ni. When the Cr content is high, on the one hand, there is enough Cr in the alloy to diffuse to the surface for the oxidation reaction, which makes the Cr_2O_3 grains grow continuously; on the other hand, the replacement reaction $2Cr+3NiO= Cr_2O_3+3Ni$ may occur, which reduces the initially formed NiO, so that a single oxide film consisting of Cr_2O_3 may be formed. The formation of a complete Cr_2O_3 layer acts as a good barrier to the diffusion of O and Ni. However, cracks are also created within the Cr_2O_3 layer on the Cr40 surface, providing a pathway for the inward diffusion of O.

Table 2 EDS results of different areas in Fig.5 (wt%)

Area	1	2	3	4	5	6	7
O	21.8	19.3	28.1	21.3	32.2	31.8	29.0
Ni	34.7	67.3	25.0	68.0	2.6	1.9	1.8
Cr	43.5	13.5	46.9	10.7	65.2	66.3	69.2

2.3 Hot corrosion characteristics

2.3.1 Corrosion products and corrosion mass loss per unit area

The XRD analysis results of corrosion products of three Ni-Cr alloy cladding layers exposed to mixed salt of Na_2SO_4 +25wt% K_2SO_4 at 600 °C for 144 h are shown in Fig. 6a. Similarly, γ-Ni solid solution is detected in three cladding layers. Various corrosion products such as NiO, Ni_3S_2 and Cr_2O_3 are detected on the surface of Cr10. In addition to NiO and Cr_2O_3, CrS is also formed on the surface of Cr20. However, almost only Cr_2O_3 forms on the surface of Cr40. The specific distribution of corrosion products on the surface of the cladding layers is presented in Sections 2.3.2 and 2.3.3 below. Fig.6b shows the corrosion mass loss of three cladding layers. It can be seen that Cr40 presents the minimum corrosion mass loss, but the corrosion resistance of Cr10 is the worst, whose corrosion mass loss is approximately 4.54 times higher than that of Cr40 and 3.59 times higher than that of Cr20. Cr40 exhibits the best corrosion resistance because of

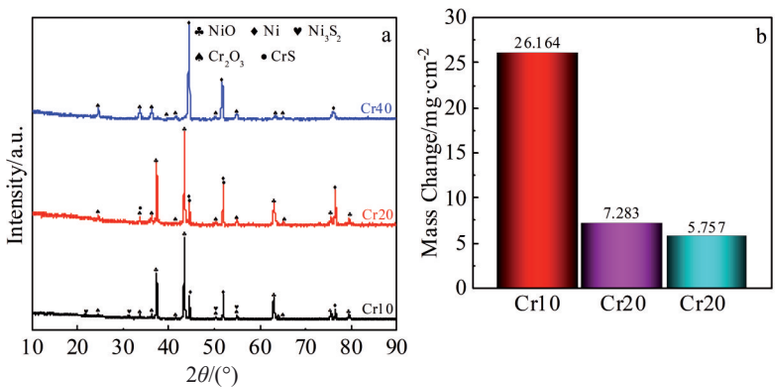

Fig.6 XRD patterns of corrosion products (a) and corrosion mass loss per unit area (b)

the formation of a dense Cr_2O_3 dominated oxide layer on the surface. However, Cr10 and Cr20 are not enough to maintain the presence of a continuous and dense Cr_2O_3 dominated oxide layer for a long time due to the low Cr content, thus forming Ni and Cr sulfides and showing poor corrosion resistance.

2.3.2 Surface morphology of corrosion products

Fig. 7 shows the surface morphology of the corrosion products of three Ni-Cr alloy cladding layers corroded at 600 °C for 144 h in Na_2SO_4+25wt% K_2SO_4 at 600 °C. The results of EDS analysis for the corresponding locations are listed in Table 3. It can be seen that Cr10 undergoes severe corrosion, the surface is uneven, and the corrosion products show a large number of cracks and severe spalling. According to the EDS results, the flatter corrosion products (areas 1 and 2) are dominated by Ni and O, and it is determined as NiO combined with the XRD results. After magnification of the spalling location, it can be found that there are a large number of sulfide particles of Ni. The corrosion products on the surface of Cr20 are obviously denser, but there is still delamination and detachment. The outer corrosion product is magnified as shown in Fig. 7b$_1$, there are clusters of corrosion products, and according to the EDS analysis results of areas 4 and 5, the outer layer is found to be an oxide of Ni. The outer Ni-rich oxide layer peels off to reveal the corrosion products as shown in area 6, where Cr content is elevated, containing a large amount of Ni and O, combined with XRD results it is

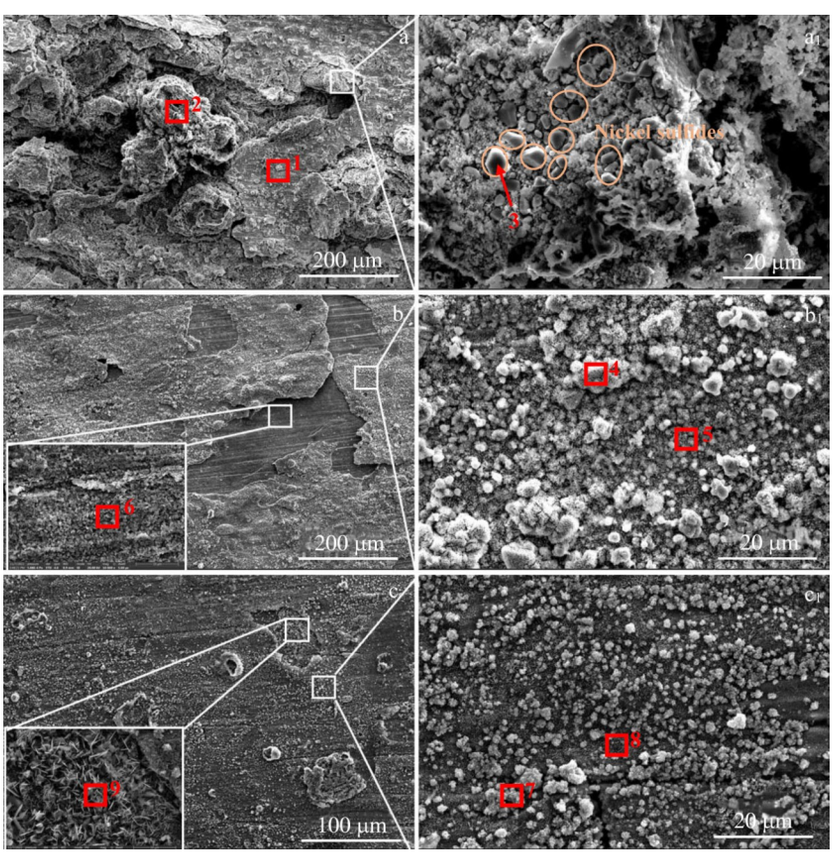

Fig.7 Surface morphologies of corrosion products of three Ni-Cr alloy cladding layers: (a, a$_1$) Cr10, (b, b$_1$) Cr20, and (c, c$_1$) Cr40

Table 3 EDS results of different areas in Fig. 7 (wt%)

Area	1	2	3	4	5	6	7	8	9
O	14.5	17.5	0.6	26.7	23.4	23.3	31.2	42.5	37.7
Na	0.4	0.3	0.2	1.0	0.2	1.6	0.6	0.8	1.6
S	0.9	0.7	24.3	1.0	1.0	0.9	0.6	0.4	0.9
K	0.7	0.4	0.4	1.1	1.0	0.9	0.8	0.7	1.4
Cr	5.7	3.6	1.0	3.7	3.6	13.3	58.2	52.6	54.7
Ni	77.7	77.6	73.5	66.5	70.8	60.1	8.7	3.0	3.8

determined as $NiCr_2O_4$. The spalling area of corrosion products on the surface of Cr40 is significantly smaller, and according to the EDS results, the outer layer (areas 7 and 8) is almost all Cr and O, while the composition of the exposed needle-like corrosion products at the spalling area is similar to that of the outer layer. Therefore, the outer layer of Cr40 consists mainly of dense Cr_2O_3 layer, and thus Cr40 exhibits the best hot corrosion resistance.

2.3.3 Cross-sectional shape of corrosion products

Fig.8 shows the cross-sectional morphology of the three Ni-Cr alloy cladding layers after corrosion at 600 °C for 144 h in Na_2SO_4 +25wt% K_2SO_4. The results of EDS analysis for a typical region are given in Table 4. It can be seen that most of the corrosion products generated on the surface of Cr10 have come off, and the multilayer stacking of Ni oxides and Ni sulfides can be observed through the residual corrosion products (areas 1 and 2). The EDS results in area 3 show that Cr-rich oxides have been generated in the lowermost layer of the corrosion products, and severe Cr loss occurs at the location of the cladding layer next to it (area 4). Area 5 confirms that S has intruded into the Cr10 cladding layer through the corrosion product layer, generating Ni sulfides and producing an internal corrosion zone. The outer corrosion product of Cr20 is loose and porous, and the surface is dominated by Ni-rich oxides (area 6), which are interspersed with white Ni sulfide particles (area 7). Below the Ni-rich oxide layer, i. e., the location of area 8, Cr_2O_3 is generated. However, the more severe internal corrosion area located below indicates that it fails to produce a good protective effect. In the internal corrosion zone, compounds of S and Cr are found in area 9, which are judged to be CrS in combination with XRD results, while a dense Cr_2O_3 protective layer is generated on the surface of Cr40, and no significant internal corrosion is observed below. Thus, Cr40 in Fig. 8 demonstrates minimal mass loss per unit area.

During hot corrosion experiment, $(Na,K)_2SO_4$ can produce free S in the presence of certain reducing agents, and the metal sulfides generated by the reaction of S with metallic elements of the cladding layer, such as Ni and Cr, can also form

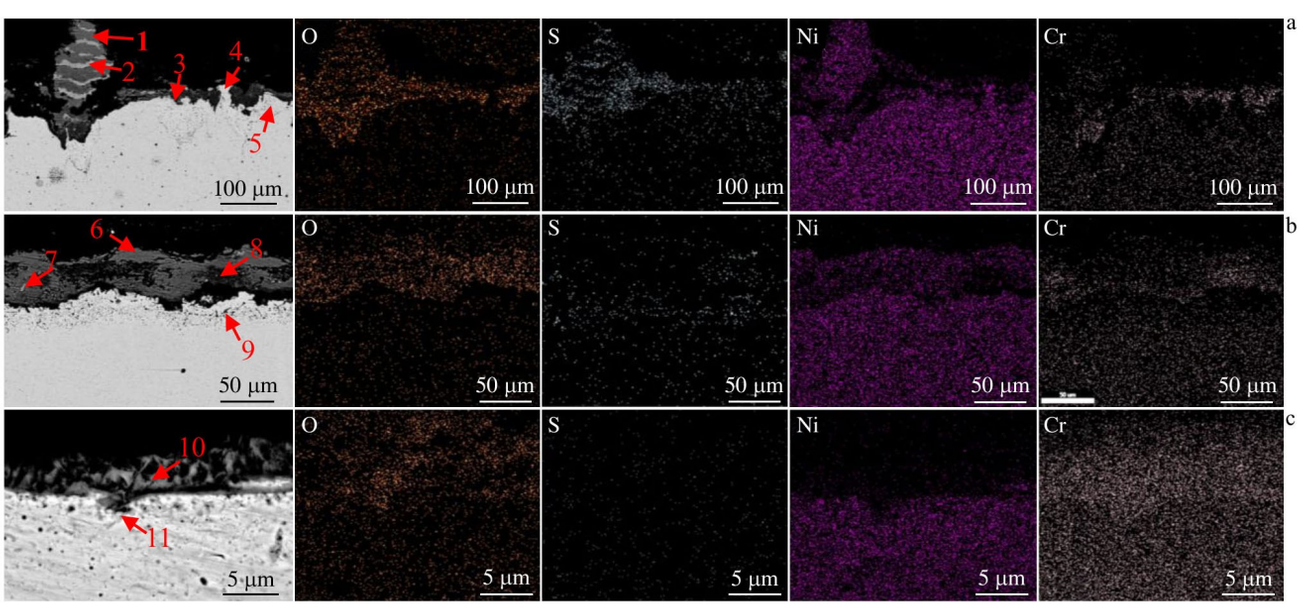

Fig.8 Cross-sectional morphologies and EDS element mappings of the three Ni-Cr alloy cladding layers: (a) Cr10, (b) Cr20, and (c) Cr40

Table 4 EDS results of different areas in Fig.8 (wt%)

Area	1	2	3	4	5	6	7	8	9	10	11
O	18.0	2.2	28.3	0.6	0.6	21.4	1.4	31.6	1.3	21.6	2.4
Na	0.4	0.2	0.2	0.3	0.5	0.2	0.4	0.2	0.3	0.2	0.3
S	2.6	20.0	2.3	0.6	25.5	0.5	26.0	1.8	38.3	0.5	0.4
K	0.7	0.4	0.6	0.4	0.4	0.5	0.3	0.4	0.5	0.5	0.5
Cr	3.5	1.0	48.7	1.3	1.6	13.4	6.3	59.7	50.8	64.5	57.2
Ni	74.8	76.3	19.8	96.7	71.5	63.9	65.6	6.3	8.8	12.7	39.2

eutectics with metallic elements with low melting points. The main reactions are as follows:

$$(Na,K)_2SO_4+3R=(Na,K)_2O+3RO+S \quad (1)$$

$$M+S=MS \quad (2)$$

$$(Na,K)_2SO_4+3MS=(Na,K)_2O+3MO+4S \quad (3)$$

where R is some kind of reducing agent and M is a metal element. Through the above reaction, the protective oxide layer generated on the surface of the cladding layer can be destroyed, making it easier for O, S, etc to invade from the outside, leading to accelerated corrosion.

For the three Ni-Cr alloy cladding layers studied in this work, the main reason for its heat-resistant corrosion relies on the formation of a denser layer of Cr_2O_3 on the surface of the cladding layer. And the presence of $(Na, K)_2O$ will further react with the protective oxide of Cr, the formation of sulfides or chromates makes it impossible to form a protective oxide layer, which is the main reason for more serious corrosion, as follows:

$$Cr_2O_3+2(Na,K)_2O+3/2O_2=2(Na,K)_2CrO_4 \quad (4)$$

As an example of the damage from the Na_2SO_4 in the mixed salt used in this experiment to cladding layer, due to a large amount of Ni in the cladding layer, the following reaction occurs:

$$Na_2SO_4+9/2Ni=Na_2O+3NiO+1/2Ni_3S_2 \quad (5)$$

Since Cr also exists in the cladding layer, there is also a simultaneous reaction:

$$Na_2O+1/2Cr_2O_3+3/4O_2=Na_2CrO_4 \quad (6)$$

For Cr10, due to the low Cr content, it is clear from Fig.4 and Fig.5 that the oxides remaining on the surface are mainly NiO. S forms a low-melting point co-crystal of metal and metal sulfide through defects with Ni in the cladding layer, in the following reaction equations:

$$Ni+S=NiS \quad (7)$$

$$Ni+NiS=Ni\cdot NiS \quad (8)$$

$$2Ni\cdot NiS+O_2=2NiO+NiS \quad (9)$$

As the corrosion gradually proceeds, on the Cr10 surface, corrosion products appear in the form of Ni oxide and Ni sulfide, showing lamellar stacking distribution. In addition, there is also a reaction:

$$2Cr+Ni_2S_3=2CrS+3Ni \quad (10)$$

And CrS is also found in the corrosion products of the Cr20 surface. With the destruction of Cr_2O_3 by Eq. (6), the Cr content in the Cr20 cladding layer is not sufficient to maintain a continuous Cr_2O_3 layer, allowing O and S to continuously invade, and bringing about severe internal corrosion. When the Cr content is increased to 40wt%, the Cr40 cladding layer maintains good hot corrosion resistance in Na_2SO_4 +25wt% K_2SO_4 because it can form a dense oxide film Cr_2O_3 relatively quickly and provide sufficient Cr.

3 Conclusions

1) The main phase of Ni-Cr alloy cladding layer with different Cr contents is γ-Ni solid solution with uniform microstructure distribution and no obvious precipitation phase.

2) The high-temperature oxidation resistance of the cladding layer is enhanced with the increase in Cr content. The oxidation products on the surface of Cr10 are mainly NiO, the oxide layer is very easy to detach, and the internal oxidation is serious. The outermost oxidation product of Cr20 is $NiCr_2O_4$, and that of the inner layer is Cr_2O_3. The formation of a single Cr_2O_3 layer on the surface of Cr40 provides a good barrier to the diffusion of O and Ni.

3) The increase in Cr content significantly affects the hot corrosion performance of the cladding layer in the mixed sulfate salt. The corrosion product layer on the surface of Cr10 exhibits no protective effect, where NiO and Ni_3S_2 show a lamellar stacking distribution. The surface of Cr20 is dominated by the Ni oxide, the Cr_2O_3 layer is destroyed, and the internal corrosion is serious, generating CrS. A single protective layer of dense Cr_2O_3 is generated on the surface of Cr40, efficiently preventing further corrosion.

References

1 Skrifvars B J, Westn-Karlsson M, Hupa M *et al. Corrosion Science*[J], 2010, 52: 1011

2 Hwang J Y, Neira A, Scharf T W *et al. Scripta Materialia*[J], 2008, 59: 487

3 Chen Y, Lu F G, Zhang K *et al. Carbon*[J], 2016, 107: 361

4 Bryskin B, Kostylev A, Pokrovsky J. *JOM*[J], 2012, 64(6): 682

5 Verma A, Wanderka N, Singh J B *et al. Journal of Alloys & Compounds*[J], 2014, 586(6): 561

6 Verma A, Wanderka N, Singh J B *et al. Ultramicroscopy*[J], 2013, 132: 227

7 Karmazin L, Krejci J, Zeman J. *Materials Science and Engineering A*[J], 1994, 183: 103

8 Bousser E, Martinu L, Klemberg Sapieha J. *Surface and Coatings Technology*[J], 2014, 257: 165

9 Dobrzanski L A, Lukaszkowicz K. *Journal of Materials Processing Technology*[J], 2004, 157: 317

10 Wu Wangping, Chen Zhaofeng, Liu Yon. *Plasma Science and Technology*[J], 2012,14(10): 909

11 Song Y. *Study of Pulse Plating and Reaction Mechanism of Trivalent Chromium Deposition Process*[D]. New York: Clarkson University, 2000

12 Hu Y J, Wang Z X, Pang M. *Materials Today Communications*[J], 2022, 31: 103 357

13 Yuan Wuyan, Li Ruifeng, Chen Zhaohui *et al. Surface and Coatings Technology*[J], 2021, 405: 126 582

14 Wang X Y, Liu Z D, Li J Y *et al. Optik*[J], 2022, 270: 169 930

15 Liu C C, Liu Z D, Gao Y *et al. Applied Surface Science*[J], 2022, 578: 152 061

16 Yang Y, Li Y, Liang Z *et al. Surface and Coatings Technology*[J], 2021, 421: 127 424

17 Liu S, Liu Z, Wang Y *et al. Corrosion Science*[J], 2014, 83: 396

18 Ul-Hamid A. *Materials Chemistry and Physics*[J], 2003, 80(1): 135

19 Liu Z, Gao W, Dahm K L. *Acta Materialia*[J], 1998, 46(5): 1691

20 Zhang X, Zhou J, Liu C *et al. International Journal of Refractory Metals & Hard Materials*[J], 2019, 80: 123

不同Cr含量的Ni-Cr合金熔覆层的高温氧化和热腐蚀特性

陈珊珊，刘宗德，潘朝阳，刘福来，付云娣

(华北电力大学 电站能量传递转化与系统教育部重点实验室，北京 102206)

摘 要：采用激光熔覆技术制备了Cr质量分数为10%、20%和40%的Ni-Cr合金熔覆层，研究了其在900 ℃下的高温氧化特性和600 ℃下Na_2SO_4+25% K_2SO_4混合盐中热腐蚀特性。结果表明，Cr含量对熔覆层的高温特性起着关键作用。提高Cr含量对提升熔覆层抗硫酸盐诱导的热腐蚀能力比提升抗循环高温氧化能力更有效。Cr40涂层抗高温氧化和热腐蚀性能最佳。Cr10的氧化产物以NiO为主，极易脱落，内部氧化严重。虽然Cr40表面可以形成单一的Cr_2O_3层，但热应力和生长应力引起的富Cr氧化物内部开裂，使Cr40的抗循环高温氧化能力仅略好于Cr20。面对热腐蚀时，Cr10表面呈现层状NiO和Ni_3S_2叠层分布的腐蚀产物，内部腐蚀区也生成了Ni的硫化物。Cr20表面Cr_2O_3层被破坏，内部腐蚀严重，生成了CrS。Cr40表面生成了致密的Cr_2O_3保护层，有效地防止了进一步腐蚀。

关键词：Ni-Cr合金；激光熔覆技术；高温氧化；高温硫酸盐腐蚀

作者简介：陈珊珊，女，1987年生，博士，华北电力大学电站能量传递转化与系统教育部重点实验室，北京 102206，电话：010-61772277，E-mail：10602054@ncepu.edu.cn